THE JOURNAL OF BIOLOGICAL CHEMISTRY VOL. 289, NO. 16, pp. 11175–11182, April 18, 2014
© 2014 by The American Society for Biochemistry and Molecular Biology, Inc. Published in the U.S.A.

Disulfide Cross-linking of Transport and Trimerization Domains of a Neuronal Glutamate Transporter Restricts the Role of the Substrate to the Gating of the Anion Conductance*

Received for publication, January 14, 2014, and in revised form, February 17, 2014 Published, JBC Papers in Press, February 28, 2014, DOI 10.1074/jbc.M114.550277

Mustafa Shabaneh[1], **Noa Rosental**[1], **and Baruch I. Kanner**[2]

From the Department of Biochemistry and Molecular Biology, Institute for Medical Research Israel-Canada, Hebrew University Hadassah Medical School, Jerusalem 91120, Israel

Background: Glutamate transporters gate anion conductance and structures of homologues are available.
Results: Disulfide cross-linking of transport and trimerization domains leaves the anion conductance intact.
Conclusion: The anion conducting conformation of brain glutamate transporters is associated with a limited inward movement of the transport domain.
Significance: The new insights into ion conducting modes may be relevant for other transporters.

Excitatory amino acid transporters remove synaptically released glutamate and maintain its concentrations below neurotoxic levels. EAATs also mediate a thermodynamically uncoupled substrate-gated anion conductance that may modulate cell excitability. A structure of an archeal homologue, which reflects an early intermediate on the proposed substrate translocation path, has been suggested to be similar to an anion conducting conformation. To probe this idea by functional studies, we have introduced two cysteine residues in the neuronal glutamate transporter EAAC1 at positions predicted to be close enough to form a disulfide bond only in outward-facing and early intermediate conformations of the homologue. Upon treatment of *Xenopus laevis* oocytes expressing the W441C/K269C double mutant with dithiothreitol, radioactive transport was stimulated >2-fold but potently inhibited by low micromolar concentrations of the oxidizing reagent copper(II)(1,10-phenanthroline)$_3$. The substrate-induced currents by the untreated double mutant, reversed at approximately −20 mV, close to the reversal potential of chloride, but treatment with dithiothreitol resulted in transport currents with the same voltage dependence as the wild type. It appears therefore that in the oocyte expression system the introduced cysteine residues in many of the mutant transporters are already cross-linked and are only capable of mediating the substrate-gated anion conductance. Reduction of the disulfide bond now allows these transporters to execute the full transport cycle. Our functional data support the idea that the anion conducting conformation of the neuronal glutamate transporter is associated with an early step of the transport cycle.

In the brain, the signaling by glutamate is terminated by transporters that remove this excitatory neurotransmitter from the cleft into the cells surrounding the synapse. Glutamate transport is an electrogenic process (1, 2) in which the transmitter is cotransported with three sodium ions and a proton (3, 4) followed by the countertransport of one potassium ion per transported glutamate molecule (5–7). Glutamate transporters mediate two types of substrate-induced steady-state current: an inward rectifying current reflecting electrogenic sodium-coupled glutamate translocation, and an "uncoupled" sodium-dependent current, which is carried by chloride ions and further activated by substrates of the transporter (8–10). It has been proposed that this anion conductance is important to limit cell excitability by restricting membrane depolarization and thereby additional glutamate release (8, 11).

Several crystal structures of a glutamate transporter homologue, Glt_{Ph}, from the archeon *Pyrococcus horikoshii* are now available (12–15). The structure reveals a trimer with a permeation pathway through each of the protomers, indicating that the protomer is the functional unit. This is also the case for the eukaryotic glutamate transporters (16–19). The protomer contains eight transmembrane domains (TMs)[3] and two oppositely oriented reentrant loops, one between domains 6 and 7 (HP1) and the other between domains 7 and 8 (HP2) (12). This unusual topology is in excellent agreement with that inferred from biochemical studies on the brain transporters (20–22). Moreover, many of the amino acid residues of the brain transporters that have been inferred to be important in the interaction with sodium (23, 24), potassium (7, 25), and glutamate (26, 27) are facing toward the binding pocket. Thus, the Glt_{Ph} structures represent excellent models for the brain transporters.

Substrate translocation by Glt_{Ph}, as well as by the neuronal transporter EAAC1, appears to take place by an "elevator-like" mechanism (14, 28) where the transport domain, which includes HP1 and HP2 and TMs 3, 6, 7, and 8, moves relative to

* This work was supported, in whole or in part, by National Institutes of Health Grant NS 16708 from NINDS. This work was also supported by United States-Israel Binational Science Foundation Grant 2011268.
[1] Both authors contributed equally to this work.
[2] To whom correspondence should be addressed. Tel.: 972-2-6758506; Fax: 972-2-6757379; E-mail: baruch.kanner@mail.huji.ac.il.

[3] The abbreviations used are: TM, transmembrane domain; ANOVA, analysis of variance; CuPh, copper(II)(1,10-phenanthroline)$_3$.

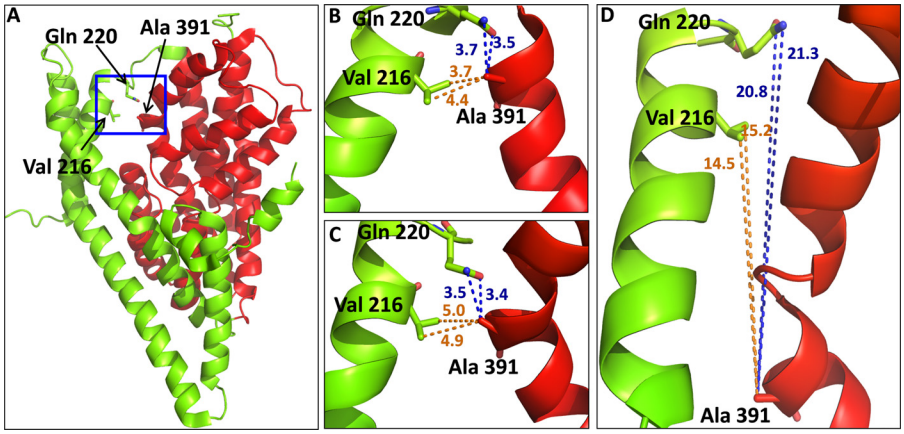

FIGURE 1. **Distances of positions in Glt_{Ph} structures, corresponding to those used for paired cysteine mutagenesis in EAAC1.** *A*, intermediate Glt_{Ph} structure (Protein Data Bank ID 3V8G) shows (*blue box*) the positions of Ala-391 (TM8) from transport domain (*red*) and Val-216 and Gln-220, respectively (TM5), from the trimerization domain (*green*). *B*—*D*, the distances between these positions are shown in the outward-facing (*B*), intermediate (*C*), and inward-facing (*D*) structures. The Glt_{Ph} residues Val-216 and Gln-220 (TM5) and Ala-291(TM8) correspond to Lys-269, Val-273, and Trp-441 from EAAC1, respectively. Distances are given in ångstroms. The figure was prepared using the PyMOL Molecular Graphics System, Version 1.5.0.4, Schrödinger, LLC.

the fixed trimerization domain (29). Comparison of outward- and inward-facing Glt_{Ph} structures shows that the transport domain traverses the membrane by approximately 15 Å during the translocation (12–14). A clue on the anion conducting mode comes from an "intermediate" Glt_{Ph} structure, where the transport domain has moved by only 3.5 Å relative to the outward-facing structure (Fig. 1*A*) (15). In contrast to the outward- and inward-facing structures, the intermediate structure shows a cavity potentially accessible to both the extracellular and cytoplasmic media (15). Because Glt_{Ph} is also capable of substrate-dependent anion conduction (30), the intermediate structure was hypothesized to be similar to the anion conducting conformation. A prediction of this idea is that if the relative movement of the transport domain will be restricted to less than 5–7 Å, transport should be abolished, but the ability of the substrate to gate the anion conductance should remain intact. Here we show that this phenotype is indeed observed in the neuronal glutamate transporter EAAC1, when cysteine residues are introduced in the extracellular parts of TM5 and 8 at positions close enough to enable the formation of a disulfide bond under oxidizing conditions in both outward-facing and intermediate conformations.

EXPERIMENTAL PROCEDURES

Generation and Subcloning of Mutants—The C-terminal histidine-tagged versions of rabbit EAAC1 (31, 32) in the vector pBluescript SK^- (Stratagene) were used as parents for site-directed mutagenesis (33, 34). This was followed by subcloning of the mutations into the His-tagged EAAC1, residing in the oocyte expression vector pOG_1 (32), using the unique restriction enzymes NsiI and StuI. The subcloned DNA fragments were sequenced between these restriction sites.

Cell Growth and Expression—HeLa cells were cultured (35), infected with the recombinant vaccinia/T7 virus vTF_{7-3} (36), and transfected with the plasmid DNA harboring the WT or mutant constructs or with the plasmid vector alone (35). Transport of D-[^{3}H]aspartate was done as described (33). Briefly, HeLa cells were plated on 24-well plates and washed with transport medium containing 150 mM NaCl, 5 mM KP_i, pH 7.4, 0.5 mM $MgSO_4$, and 0.3 mM $CaCl_2$. Each well was then incubated with 200 μl of transport medium supplemented with 0.4 μCi of the substrate D-[^{3}H]aspartate for 10 min, followed by washing, solubilization of the cells with SDS, and scintillation counting. Effects of CuPh and DTT on transport were monitored after washing the cells expressing the indicated constructs once with choline solution (150 mM choline chloride, 5 mM KP_i, pH 7.4, 0.5 mM $MgSO_4$, and 0.3 mM $CaCl_2$) followed by a 5-min preincubation with the concentrations of these reagents in the media indicated in the figure legends. The solutions of CuPh and DTT were prepared just prior to each individual experiment. In the case of CuPh this was done from a frozen aliquot of a stock solution prepared by mixing 0.4 ml of 1.25 M CuPh in water/ethanol (1:1) with 0.6 ml of 250 mM $CuSO_4$. Statistical evaluations utilized a one-way ANOVA with a *post hoc* Dunnett multiple comparison test. In the case of the effects by Cd^{2+} there was no preincubation, and D-[^{3}H]aspartate transport was measured in the presence of the indicated concentrations of Cd^{2+}.

Expression in Oocytes, Electrophysiology, and Radioactive Uptake—cRNA was transcribed using mMESSAGE-mMACHINE (Ambion) and injected into *Xenopus laevis* oocytes, which were maintained as described (24). Oocytes were placed in the recording chamber, penetrated with two agarose-cushioned micropipettes (1% 2 M KCl, resistance varied between 0.5 and 3 megohms), voltage clamped using GeneClamp 500 (Axon Instruments), and digitized using Digidata 1322 (Axon Instruments) both controlled by the pClamp9.0 suite (Axon Instruments). Voltage jumping was performed using a conventional two-electrode voltage clamp as described previously (32). The standard buffer, termed ND96, was composed of 96 mM NaCl, 2 mM KCl, 1.8 mM $CaCl_2$, 1 mM $MgCl_2$, 5 mM Na-HEPES, pH 7.5. The composition of other perfusion solutions is indicated in the figure legends. Offset voltages in chloride substitution experiments were avoided by use of an agarose bridge (1% 2 M KCl) that connected the recording chamber to the Ag/AgCl ground electrode. Before applying the DTT or CuPh, at the concentrations in the figure legends, the flow was stopped, the oocyte was unclamped, and the grounding electrode was removed. Subse-

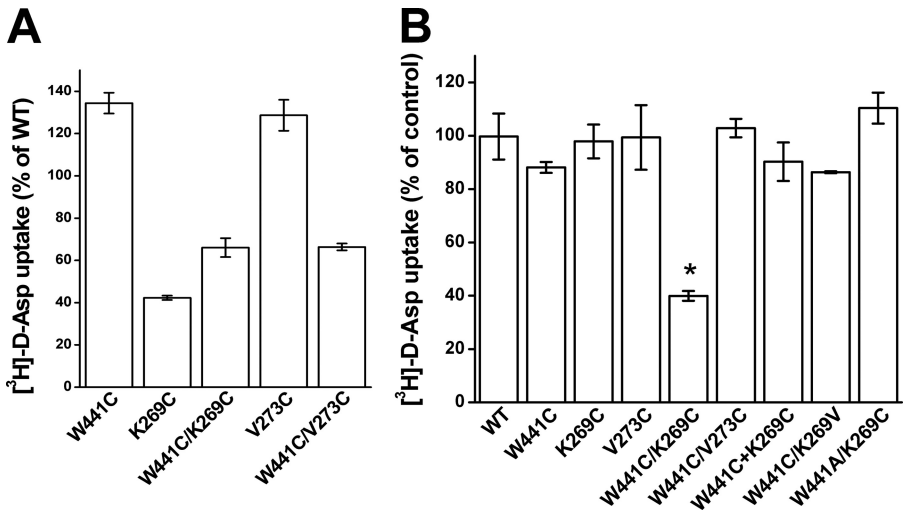

FIGURE 2. **Transport activity and the effect of CuPh on inactivation.** EAAC1-WT and the indicated mutants were transiently expressed in HeLa cells as described under "Experimental Procedures." *A*, sodium-dependent D-[^{3}H]aspartate transport was measured at room temperature for 10 min. *B*, cells were incubated in the NaCl-containing medium with or without 1 μM CuPh for 5 min at room temperature, prior to the transport measurement. For *A* the data are given as percentage of the activity of EAAC1-WT. Results represent mean ± S.E. (*error bars*) of at least three different experiments performed in quadruplicate. For *B* the data are expressed as percentage of untreated control and represent the mean ± S.E. The mean value for W441C/K269C was compared with that of EAAC1-WT using a one-way ANOVA with a *post hoc* Dunnett multiple comparison test: *, $p < 0.001$.

quently, these reagents were applied directly into the bath. After 2 or 5 min of incubation with DTT or CuPh, respectively, the oocyte was perfused with 150–200 ml of ND96 before measuring the transport currents. For radioactive uptake, eight to ten oocytes, expressing EAAC1-WT or EAAC1-W441C/K269C, were preincubated with CuPh or DTT as above, followed by an incubation for 20 min in ND96 containing D-[^{3}H]aspartate as described previously (24).

Data Analysis—All current-voltage relations represent steady-state substrate-elicited net currents ($(I_{buffer+substrate}) - (I_{buffer})$) and were analyzed by Clampfit version 8.2 or 9.0 (Axon instruments), and the data have been normalized as indicated in the figure legends.

RESULTS

Selection of Positions for Paired Cysteine Mutagenesis—To restrict the movement of the transport domain relative to the trimerization domain, we introduced a cysteine residue in each, followed by oxidative cross-linking. We searched for positions in the Glt_{Ph} structure, predicted to be close enough so that the introduced cysteine residues potentially could form a disulfide bond under oxidizing conditions. To increase the probability of accessibility to oxidizing reagents, positions at the external parts of these domains were selected. As can be seen, both Val-216 and Gln-220 from TM5 (trimerization domain) are close to Ala-391 from TM8 (transport domain) in the outward-facing (Fig. 1*B*) and intermediate structures (Fig. 1*C*). However, the paired residues are far from each other in the inward-facing structure (Fig. 1*D*). Therefore, cysteine residues were introduced at the corresponding positions of the neuronal glutamate transporter EAAC1, yielding the mutants K269C, V273C, and W441C. Because we used inhibition of D-[^{3}H]aspartate uptake by CuPh as an indirect read-out of cross-linking, the transport activity of the mutants needs to be significant. Therefore, we did not use mutant combinations involving R445C, which is the EAAC1 counterpart of Met-395 of Glt_{Ph}, located one α-helical turn "below" Ala-391 and close to Ile-213 and Val-216. Substitution of Arg-445 by serine results in very low transport rates (32), and transport activity of R445C was only 15.7 ± 5.2% of EAAC1-WT ($n = 4$). This is the reason that only W441C/K269C and W441C/V273C were considered for our subsequent studies. Because of the highly variable transporter expression in *Xenopus* oocytes, we studied the effect of CuPh and other reagents on radioactive transport in HeLa cells (but see Fig. 8 for experiments with oocytes). We used D-[^{3}H]aspartate for these studies because with this transporter substrate the background levels in the HeLa cell expression system are lower than with L-[^{3}H]aspartate or with L-[^{3}H]glutamate.

Effects of CuPh and $CdCl_2$ on Radioactive Transport in HeLa Cells—The transport activity of W441C and V273C was somewhat higher than that of EAAC1-WT (Fig. 2*A*). However, the activity of K269C and the double mutants W441C/K269C and W441C/V273C was lower, but their transport activity was nevertheless sufficient to perform reliable measurements (Fig. 2*A*). Transport by W441C/K269C was inhibited by low micromolar concentrations of CuPh. Preincubation of the cells expressing this double mutant with 1 μM CuPh resulted already in an inhibition of D-[^{3}H]aspartate transport of 60–70% (Figs. 2*B* and 3). No such inhibition was observed with cells expressing the double mutant W441C/V273C, EAAC1-WT, and the single mutants K269C and V273C (Fig. 2*B*). However, some inhibition was seen with W441C (Fig. 2*B*), but as can be seen from analysis of the concentration dependence of inhibition by CuPh, the inhibition seen with W441C was much lower than with W441C/K269C (Fig. 3). No inhibition was seen with W441A/K269C (Fig. 2*B*), indicating that the effect of CuPh on W441C/K269C is unlikely to be caused by the cross-linking of cysteine 269 with a previously buried endogenous cysteine, which became exposed as a consequence of the replacement of Trp-441 with a smaller amino acid residue. The modest inhibition seen with W441C/K269V is similar to that of W441C alone

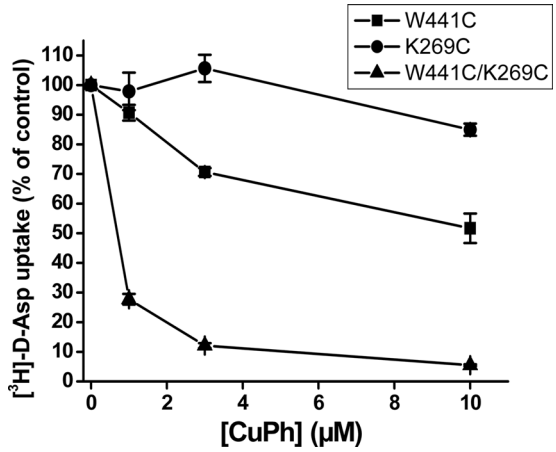

FIGURE 3. **Sensitivity of W441C/K269C to CuPh.** HeLa cells expressing the indicated mutants were preincubated in NaCl-containing medium with the indicated concentrations of CuPh for 5 min at room temperature. Subsequently the cells were washed and assayed for D-[^{3}H]aspartate transport as described in "Experimental Procedures." Values are given as percentage of activity in the absence of CuPh.

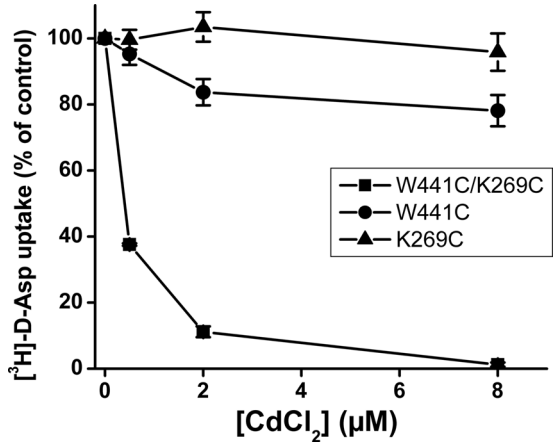

FIGURE 4. **Sensitivity of W441C/K269C to cadmium ions.** HeLa cells expressing the indicated mutants were assayed for D-[^{3}H]aspartate transport, which was measured in the presence of the indicated concentrations of Cd^{2+}.

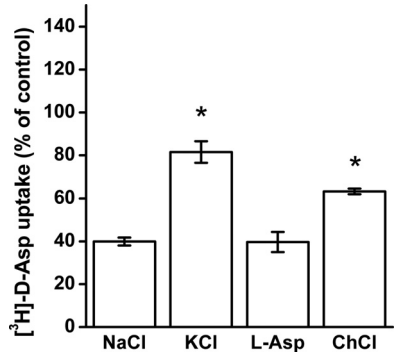

FIGURE 5. **Effect of the composition of the external medium on the inhibition of W441C/K269C by CuPh.** HeLa cells expressing W441C/K269C were preincubated in the presence or absence of 1 μM CuPh in media containing NaCl, KCl, choline chloride, and NaCl + 1 mM L-aspartate (L-Asp). Values are given as percentage of control (preincubation without CuPh in each condition) and represent the mean ± S.E. (*error bars*) of at least three different experiments done in quadruplicate. The mean values with the different conditions were compared with those from NaCl-containing medium using one-way ANOVA with a *post hoc* Dunnett multiple comparison test: *, $p < 0.001$.

(Fig. 2*B*), and thus in the background of W441C, potent inhibition only is observed with a cysteine residue present at position 269. Finally, when W441C and K269C were coexpressed using different plasmids (W441C + K269C), the same small inhibition was observed as with W441C (Fig. 2*B*), indicating that for potent inhibition the two cysteine residues need to be present on the same polypeptide chain. To examine the possibility that part of the cells expressing W441C/K269C transporters was already cross-linked, even prior to treatment with CuPh, the cells were assayed for transport after incubation with 12 mM DTT. However, this resulted only in a minor stimulation of transport activity, which was 111.2 ± 5.3% of the untreated control compared with 106.2 ± 1.2% in the case of EAAC1-WT ($n = 3$).

To provide additional evidence that positions 441 and 269 could be close in space, the ability of the W441C/K269C double mutant to form a high affinity Cd^{2+} binding site was examined. This divalent cation interacts with cysteinyl side chains (37, 38), and the affinity of the interaction is dramatically increased when the Cd^{2+} can be coordinated by two cysteines (39). Consistent with the oxidative cross-linking data, transport by W441C/K269C was also extremely sensitive to Cd^{2+} (Fig. 4). The activity of K269C was not inhibited by Cd^{2+}, at least not in the concentration range tested, whereas W441C was only slightly sensitive (Fig. 4).

The degree of cross-linking between the cysteine residues introduced at positions 269 and 441 of EAAC1 is expected to depend on the conformation of the transporters. Therefore, the preincubation step with 1 μM CuPh was done in the presence and absence of transporter ligands. The highest sensitivity was observed when the preincubation medium contained sodium, either in the presence or in the absence of the substrate L-aspartate (Fig. 5). A significant protection against the inhibition was observed in the presence of potassium, whereas intermediate sensitivity was observed when choline was present in the preincubation medium (Fig. 5).

Transport Currents by the W441C/K269C Double Mutant—The voltage dependence of the L-aspartate-induced currents by oocytes expressing W441C/K269C was found to be markedly different from those expressing EAAC1-WT (Fig. 6). In the case of EAAC1-WT, the observed substrate-induced transport currents represent the sum of the inward-rectifying current, reflecting electrogenic substrate translocation and of the reversible uncoupled substrate-gated chloride current (8–10). Consistently, the reversal potential of the total current by EAAC1-WT was much more positive than the reversal potential of chloride, which is approximately −25 mV, and the same is true for W441C and K269C (Fig. 6). Remarkably, the reversal potential of the total current by W441C/K269C was approximately −20 mV (Fig. 6), suggesting that most of this current is contributed by the uncoupled anion conductance. This idea is further supported by the fact that substitution of the extracellular chloride by the much more permeant nitrate results in a shift of the reversal potential to approximately −50 mV. Moreover, in this case much larger outward currents are observed, apparently due the increased rate of inward movement of negative charges carried by nitrate (Fig. 7*A*). Indeed, replacement of extracellular chloride by the impermeant gluconate abolishes the outward but not the inward current, at least over the range

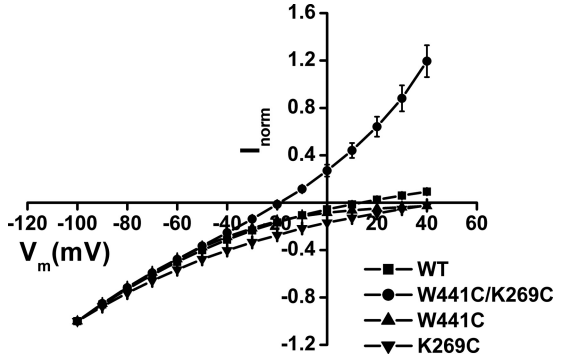

FIGURE 6. **Substrate-induced steady-state currents by EAAC1-WT and mutants.** Steady-state currents induced by 1 mM L-aspartate were measured in oocytes expressing either EAAC1-WT or the indicated mutants in a NaCl-based external medium (ND96), as described under "Experimental Procedures." The membrane voltage was stepped from a holding potential of −25 mV to voltages between −100 and +40 mV in increments of +10 mV. Each potential was held clamped for 250 ms followed by 250 ms of a potential clamped at −25 mV. Substrate-induced steady-state currents ($I_{substrate} - I_{ND96}$) from 210 to 240 ms at each potential was averaged and normalized to the current induced by 1 mM L-aspartate at −100 mV (I_{norm}). These currents were then plotted against the corresponding potential (V_m (mV)). Data are mean ± S.E. of at least three repeats. The currents at −100 mV induced by 1 mM L-aspartate ranged from −200 to −800 nA in the WT, from −550 to −700 nA in W441C, from −50 to −200 nA in K269C, and from −60 to −300 nA in W441C/K269C.

tested (Fig. 7*A*). Moreover, when the external chloride concentration was varied, the reversal potential of the currents by W441C/K269C was shifted by approximately 30 mV/3.3-fold change in [Cl^-] (Fig. 7*B*), close to the prediction from the Nernst equation.

Effects of DTT and CuPh—The major contribution of the anion conductance to the total transport current by W441C/K269C suggests that in oocytes a substantial part of the transporters is already cross-linked. Indeed, preincubation of the oocytes expressing the double mutant with DTT resulted in a marked stimulation of radioactive D-[^{3}H]aspartate transport, in contrast to EAAC1-WT (Fig. 8). In further contrast with EAAC1-WT, treatment of W441C/K269C with 10 μM CuPh resulted in inhibition of the radioactive transport (Fig. 8). Preincubation of the oocytes expressing W441C/K269C with DTT had a remarkable effect on the L-aspartate-induced currents. Namely, this resulted in a right shift of the reversal potential of the transport current by approximately 35 mV (Fig. 9*A*), which is very similar to that of EAAC1-WT (Fig. 6). This shift was reversed by subsequent treatment with CuPh (Fig. 9*A*), supporting the idea that disulfide formation between positions 269 and 441 suppresses coupled transport, but not the anion conductance. Furthermore, preincubation with DTT not only shifted the reversal potential, but also resulted in a decreased apparent affinity for L-aspartate (Fig. 9*B*).

DISCUSSION

Because the intermediate Glt_{Ph} structure shows a small cavity, which is not seen in the earlier reported outward- and inward-facing structures, it was postulated that the intermediate structure could be similar to the anion conducting mode of eukaryotic as well as of archeal glutamate transporters. This idea could explain a number of earlier characterized properties of the nature of the anion conducting mode on the brain transporters, made prior to the determination of the crystal structures from Glt_{Ph}: (i) the substrate-gated anion conductance was much less sensitive to changes in temperature than substrate transport (Q_{10} approximately 1.3 and 3, respectively) (40), indicating a smaller conformational change required for gating of the anion conductance; and (ii) modification of cysteines introduced at the extracellular side of the transport domain by charged methanethiosulfonate reagents prevented coupled transport but not the substrate-gated anion conductance (41–44). In this study we have tested a specific prediction of the hypothesis linking the intermediate structure to the anion conducting mode of the transporter, namely that oxidative cross-linking of one cysteine residue introduced in the transport domain with another from the trimerization domain may still allow the transition from outward-facing to intermediate conformation(s) (Fig. 1). However, such a maneuver is expected to prevent the full elevator-like movement to the inward-facing conformation and thus impair transport (Fig. 1).

Xenopus oocytes are an excellent tool to monitor the substrate-gated anion conductance, but because of the highly variable transporter expression in oocytes, we have used the HeLa cell system to screen for inhibition of radioactive transport in double cysteine mutants by CuPh and to perform the appropriate control experiments. Reassuringly, the inhibition of the activity of W441C/K269C by CuPh in the HeLa cell expression system (Figs. 2*B* and 3) was also observed when expressed in oocytes (Fig. 8). The high potency inhibition of transport by W441C/K269C by CuPh (Figs. 2*B* and 3) is similar to that observed with A364C/S440C from the glutamate transporter GLT-1 (45). This is in good agreement with the similar proximity of the equivalent positions in the outward-facing conformation of Glt_{Ph} with distances between the Cα atoms ranging from approximately 5 to 7 Å (12). However, much higher concentrations of the oxidant are required to inhibit the EAAC1 double mutants R61C/V420C and K55C/V420C where, in a model of inward-facing transporter, the distances between the Cα atoms are estimated to be approximately 10 Å (28). These observations suggest that the close proximity of positions 441 and 269 from EAAC1 is similar to that of their Glt_{Ph} counterparts in the outward-facing and intermediate conformations. Moreover, they reinforce the idea that Glt_{Ph} is an excellent model for the glutamate transporters from the brain. The potent inhibition of W441C/K269C by CuPh was not seen with W441C/V273C (Fig. 2*B*), even though the distance between Glt_{Ph} equivalents of positions 441 and 273 is even shorter than those between 441 and 269 (Fig. 1). A possible explanation may be that the bond angle of the cysteinyl side chain at position 269 is more conducive than that at position 273 for cross-linking with the cysteine introduced at position 441. Although the use of the degree of inhibition of transport of double cysteine mutants by CuPh as a read-out of oxidative cross-linking is an indirect measurement, its validity is supported by the potent inhibition of transport of W441C/K269C not only by CuPh (Figs. 2*B* and 3), but also by Cd^{2+} (Fig. 4).

The most potent inhibition of transport of W441C/K269C by CuPh was observed in the presence of sodium (Fig. 5). Sodium promotes the outward-facing conformation (46) and also can activate the anion conductance (47). Thus it appears that in the

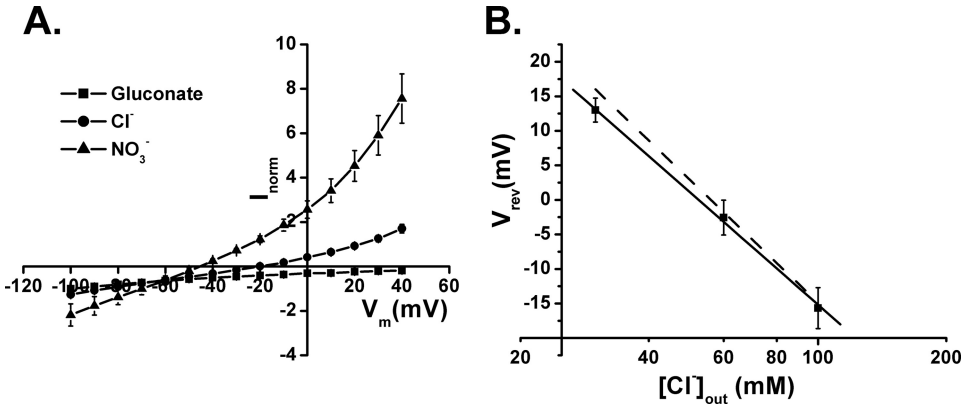

FIGURE 7. **Substrate-induced steady-state currents by W441C/K269C in the presence of different anions.** *A*, steady-state currents induced by 20 μM L-aspartate were measured in oocytes expressing W441C/K269C in ND96 without or with isosmotic replacement of the chloride by gluconate or of 20 mM chloride by nitrate, as indicated. *B*, perfusion media with varying chloride concentrations (gluconate substitution) were used, and the reversal potential was plotted as a function of the chloride concentration, using the same voltage protocol described in the legend to Fig. 6. The *dashed line* gives the predicted chloride dependence of the reversal potential according to the Nernst equation for chloride. The currents at −100 mV ranged from −200 to −250 nA.

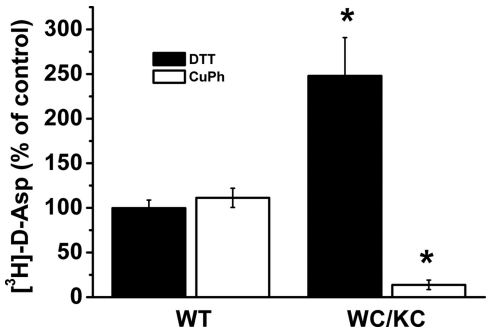

FIGURE 8. **Radioactive transport by oocytes expressing W441C/K269C.** Transport of D-[^{3}H]aspartate was done after preincubation with 12 mM DTT or 10 μM CuPh, as described under "Experimental Procedures." Results, mean ± S.E. (*error bars*), are given as percentage of untreated controls from three experiments using 8–10 oocytes, after correction for the values obtained with uninjected oocytes. The radioactive uptake ranged from 9.1 to 40.4 and 14.2 to 19.1 pmol of D-[^{3}H]aspartate/oocyte/20 min for EAAC1-WT and W441C/K269C, respectively. Values are given as percentage of control (preincubation without any additions) and represent the mean ± S.E. of at least three different experiments. The mean values with the different conditions were compared with those of the untreated control using one-way ANOVA with a *post hoc* Dunnett multiple comparison test: *, $p < 0.05$.

presence of sodium, the transporter preferentially populates the outward-facing and anion conducting states, in both of which positions 269 and 441 are close enough to form a disulfide bridge. The increased anion conductance by substrate is apparently due to a higher probability to reach the anion conducting state. Probably glutamate does not further increase the sensitivity of transport of W441C/K269C to CuPh (Fig. 5) because the increased probability to reach the anion conducting state is offset by translocation to the inward-facing state.

Transport in oocytes expressing W441C/K269C is markedly stimulated by DTT (Fig. 8). Therefore, it appears that a substantial part of these transporters is already cross-linked without pretreatment with CuPh. The transport currents by oocytes expressing the double mutant reverse close to the reversal potential of chloride (Fig. 6). This indicates that the substrate-gated anion conductance is the main component of the total current. Treatment of these transporters with DTT result in a shift the reversal potential to values similar to those observed with EAAC1-WT (Figs. 6 and 9*A*), whereas subsequent treatment with CuPh restored the original voltage dependence. These observations indicate that the cross-linked form of W441C/K269C can mediate the substrate-gated anion conductance, but not substrate transport. Nevertheless, the double mutant is capable of radioactive transport (Fig. 8). Therefore, the question can be raised as to why in the case of "native" W441C/K269C, the reversal potential is very similar to that of chloride, even though it can mediate coupled transport. A likely explanation is that the probability of cross-linked transporters to visit the anion conducting mode is substantially larger than that of non-cross-linked transporters. Therefore, in a mixture of cross-linked and non-cross-linked transporters, the contribution of the anion conductance to the total current will be much larger than in non-cross-linked transporters so that the reversal potential of the total current is expected to be close to that of chloride. Indeed, sulfhydryl modification of a cysteine residue introduced into the HP2 loop restricted the transporters to the anion conducting state with markedly increased currents (42).

Because kinetic experiments indicate that the onset of the anion conductance is delayed compared with coupled transport, it has been proposed that the substrate-induced anion conductance represents a conformation that is not an obligate intermediate of the transport cycle. Rather, it is connected to the main cycle by an early side step from the fully loaded outward-facing transporter (40, 47–49). Further support for this idea comes from observations that in EAAC1 transport requires either sodium or lithium, whereas the anion conductance strictly depends on sodium (24). If the intermediate structure reflects a conformation on the main transport path, the anion conducting conformation is apparently very similar because the disulfide bridge between cysteine residues introduced at positions 441 and 269 still enables the transporter to reach the anion conducting state. At the present time we do not have a satisfactory explanation for the decrease of the apparent affinity of the transport currents of W441C/K269C by DTT (Fig. 9*B*).

Interestingly, removal of the positive charge at position 445, by mutation of Arg-445 of EAAC1 to neutral residues resulted in the appearance of a glutamate-gated cation conductance (32). Arg-445 is located on the path leading from the extracel-

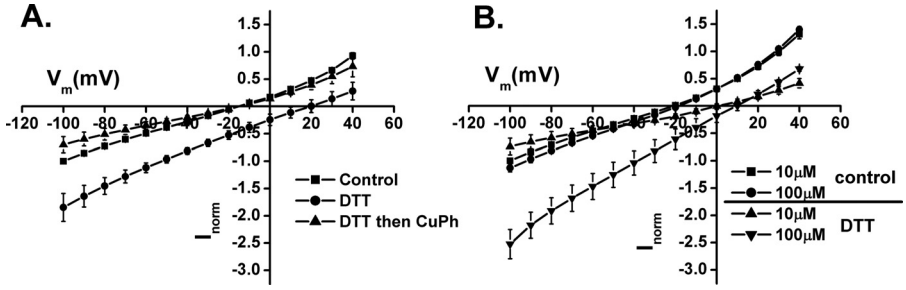

FIGURE 9. **Voltage dependence of substrate-induced currents before and after DTT treatment.** *A*, voltage dependence of the currents induced by 100 μM L-aspartate in oocytes expressing W441C/K269C before (control) and after treatment with 12 mM DTT and after DTT application followed by 10 μM CuPh. *B*, voltage dependence of currents before and after treatment with 12 mM DTT induced by 10 or 100 μM L-aspartate. The incubations were done as described under "Experimental Procedures." The currents at −100 mV ranged from −60 to −200 nA.

lular medium to the proposed ion conducting cavity (15). The role of Arg-445 as a determinant of anion selectivity is consistent with the idea that the intermediate structure is very similar to the conformation mediating the anion conducting leak. It is well known that leak pathways/uncoupled currents also occur in other transporters (see for instance Refs. 50–52). Therefore, the combination of structural information and functional studies on selected mutants, as used here, may provide important insights into the nature of the conducting states in other transporters as well.

Acknowledgment—We thank Assaf Ben-Yona for the preparation of Fig. 1.

REFERENCES

1. Kanner, B. I., and Sharon, I. (1978) Active transport of L-glutamate by membrane vesicles isolated from rat brain. *Biochemistry* **17,** 3949–3953
2. Brew, H., and Attwell, D. (1987) Electrogenic glutamate uptake is a major current carrier in the membrane of axolotl retinal glial cells. *Nature* **327,** 707–709
3. Zerangue, N., and Kavanaugh, M. P. (1996) Flux coupling in a neuronal glutamate transporter. *Nature* **383,** 634–637
4. Levy, L. M., Warr, O., and Attwell, D. (1998) Stoichiometry of the glial glutamate transporter GLT-1 expressed inducibly in a Chinese hamster ovary cell line selected for low endogenous Na^+-dependent glutamate uptake. *J. Neurosci.* **18,** 9620–9628
5. Kanner, B. I., and Bendahan, A. (1982) Binding order of substrates to the sodium and potassium ion coupled L-glutamic acid transporter from rat brain. *Biochemistry* **21,** 6327–6330
6. Pines, G., and Kanner, B. I. (1990) Counterflow of L-glutamate in plasma membrane vesicles and reconstituted preparations from rat brain. *Biochemistry* **29,** 11209–11214
7. Kavanaugh, M. P., Bendahan, A., Zerangue, N., Zhang, Y., and Kanner, B. I. (1997) Mutation of an amino acid residue influencing potassium coupling in the glutamate transporter GLT-1 induces obligate exchange. *J. Biol. Chem.* **272,** 1703–1708
8. Fairman, W. A., Vandenberg, R. J., Arriza, J. L., Kavanaugh, M. P., and Amara, S. G. (1995) An excitatory amino acid transporter with properties of a ligand-gated chloride channel. *Nature* **375,** 599–603
9. Wadiche, J. I., Amara, S. G., and Kavanaugh, M. P. (1995) Ion fluxes associated with excitatory amino acid transport. *Neuron* **15,** 721–728
10. Arriza, J. L., Eliasof, S., Kavanaugh, M. P., and Amara, S. G. (1997) Excitatory amino acid transporter 5, a retinal glutamate transporter coupled to a chloride conductance. *Proc. Natl. Acad. Sci. U.S.A.* **94,** 4155–4160
11. Picaud, S., Larsson, H. P., Wellis, D. P., Lecar, H., and Werblin, F. (1995) Cone photoreceptors respond to their own glutamate release in the tiger salamander. *Proc. Natl. Acad. Sci. U.S.A.* **92,** 9417–9421
12. Yernool, D., Boudker, O., Jin, Y., and Gouaux, E. (2004) Structure of a glutamate transporter homologue from *Pyrococcus horikoshii*. *Nature* **431,** 811–818
13. Boudker, O., Ryan, R. M., Yernool, D., Shimamoto, K., and Gouaux, E. (2007) Coupling substrate and ion binding to extracellular gate of a sodium-dependent aspartate transporter. *Nature* **445,** 387–393
14. Reyes, N., Ginter, C., and Boudker, O. (2009) Transport mechanism of a bacterial homologue of glutamate transporters. *Nature* **462,** 880–885
15. Verdon, G., and Boudker, O. (2012) Crystal structure of an asymmetric trimer of a bacterial glutamate transporter homolog. *Nat. Struct. Mol. Biol.* **19,** 355–357
16. Koch, H. P., and Larsson, H. P. (2005) Small-scale molecular motions accomplish glutamate uptake in human glutamate transporters. *J. Neurosci.* **25,** 1730–1736
17. Grewer, C., Balani, P., Weidenfeller, C., Bartusel, T., Tao, Z., and Rauen, T. (2005) Individual subunits of the glutamate transporter EAAC1 homotrimer function independently of each other. *Biochemistry* **44,** 11913–11923
18. Leary, G. P., Stone, E. F., Holley, D. C., and Kavanaugh, M. P. (2007) The glutamate and chloride permeation pathways are colocalized in individual neuronal glutamate transporter subunits. *J. Neurosci.* **27,** 2938–2942
19. Koch, H. P., Brown, R. L., and Larsson, H. P. (2007) The glutamate-activated anion conductance in excitatory amino acid transporters is gated independently by the individual subunits. *J. Neurosci.* **27,** 2943–2947
20. Grunewald, M., Bendahan, A., and Kanner, B. I. (1998) Biotinylation of single cysteine mutants of the glutamate transporter GLT-1 from rat brain reveals its unusual topology. *Neuron* **21,** 623–632
21. Grunewald, M., and Kanner, B. I. (2000) The accessibility of a novel reentrant loop of the glutamate transporter GLT-1 is restricted by its substrate. *J. Biol. Chem.* **275,** 9684–9689
22. Slotboom, D. J., Sobczak, I., Konings, W. N., and Lolkema, J. S. (1999) A conserved serine-rich stretch in the glutamate transporter family forms a substrate-sensitive reentrant loop. *Proc. Natl. Acad. Sci. U.S.A.* **96,** 14282–14287
23. Zhang, Y., and Kanner, B. I. (1999) Two serine residues of the glutamate transporter GLT-1 are crucial for coupling the fluxes of sodium and the neurotransmitter. *Proc. Natl. Acad. Sci. U.S.A.* **96,** 1710–1715
24. Borre, L., and Kanner, B. I. (2001) Coupled, but not uncoupled, fluxes in a neuronal glutamate transporter can be activated by lithium ions. *J. Biol. Chem.* **276,** 40396–40401
25. Zhang, Y., Bendahan, A., Zarbiv, R., Kavanaugh, M. P., and Kanner, B. I. (1998) Molecular determinant of ion selectivity of a (Na^+ + K^+)-coupled rat brain glutamate transporter. *Proc. Natl. Acad. Sci. U.S.A.* **95,** 751–755
26. Bendahan, A., Armon, A., Madani, N., Kavanaugh, M. P., and Kanner, B. I. (2000) Arginine 447 plays a pivotal role in substrate interactions in a neuronal glutamate transporter. *J. Biol. Chem.* **275,** 37436–37442
27. Teichman, S., and Kanner, B. I. (2007) Aspartate 444 is essential for productive substrate interactions in a neuronal glutamate transporter. *J. Gen. Physiol.* **129,** 527–539
28. Crisman, T. J., Qu, S., Kanner, B. I., and Forrest, L. R. (2009) Inward-facing conformation of glutamate transporters as revealed by their inverted-topology structural repeats. *Proc. Natl. Acad. Sci. U.S.A.* **106,** 20752–20757
29. Groeneveld, M., and Slotboom, D. J. (2007) Rigidity of the subunit interfaces of the trimeric glutamate transporter GltT during translocation. *J.*

Mol. Biol. **372,** 565–570
30. Ryan, R. M., and Mindell, J. A. (2007) The uncoupled chloride conductance of a bacterial glutamate transporter homolog. *Nat. Struct. Mol. Biol.* **14,** 365–371
31. Kanai, Y., and Hediger, M. A. (1992) Primary structure and functional characterization of a high-affinity glutamate transporter. *Nature* **360,** 467–471
32. Borre, L., and Kanner, B. I. (2004) Arginine 445 controls the coupling between glutamate and cations in the neuronal transporter EAAC-1. *J. Biol. Chem.* **279,** 2513–2519
33. Pines, G., Zhang, Y., and Kanner, B. I. (1995) Glutamate 404 is involved in the substrate discrimination of GLT-1, a (Na^+ + K^+)-coupled glutamate transporter from rat brain. *J. Biol. Chem.* **270,** 17093–17097
34. Kunkel, T. A., Roberts, J. D., and Zakour, R. A. (1987) Rapid and efficient site-specific mutagenesis without phenotypic selection. *Methods Enzymol.* **154,** 367–382
35. Keynan, S., Suh, Y. J., Kanner, B. I., and Rudnick, G. (1992) Expression of a cloned γ-aminobutyric acid transporter in mammalian cells. *Biochemistry* **31,** 1974–1979
36. Fuerst, T. R., Niles, E. G., Studier, F. W., and Moss, B. (1986) Eukaryotic transient-expression system based on recombinant vaccinia virus that synthesizes bacteriophage T7 RNA polymerase. *Proc. Natl. Acad. Sci. U.S.A.* **83,** 8122–8126
37. Pérez-Garcia, M. T., Chiamvimonvat, N., Marban, E., and Tomaselli, G. F. (1996) Structure of the sodium channel pore revealed by serial cysteine mutagenesis. *Proc. Natl. Acad. Sci. U.S.A.* **93,** 300–304
38. Glusker, J. P. (1991) Structural aspects of metal liganding to functional groups in proteins. *Adv. Protein Chem.* **42,** 1–76
39. Bénitah, J. P., Tomaselli, G. F., and Marban, E. (1996) Adjacent pore-lining residues within sodium channels identified by paired cysteine mutagenesis. *Proc. Natl. Acad. Sci. U.S.A.* **93,** 7392–7396
40. Wadiche, J. I., and Kavanaugh, M. P. (1998) Macroscopic and microscopic properties of a cloned glutamate transporter/chloride channel. *J. Neurosci.* **18,** 7650–7661
41. Seal, R. P., Shigeri, Y., Eliasof, S., Leighton, B. H., and Amara, S. G. (2001) Sulfhydryl modification of V449C in the glutamate transporter EAAT1 abolishes substrate transport but not the substrate-gated anion conductance. *Proc. Natl. Acad. Sci. U.S.A.* **98,** 15324–15329
42. Borre, L., Kavanaugh, M. P., and Kanner, B. I. (2002) Dynamic equilibrium between coupled and uncoupled modes of a neuronal glutamate transporter. *J. Biol. Chem.* **277,** 13501–13507
43. Ryan, R. M., and Vandenberg, R. J. (2002) Distinct conformational states mediate the transport and anion channel properties of the glutamate transporter EAAT-1. *J. Biol. Chem.* **277,** 13494–13500
44. Shachnai, L., Shimamoto, K., and Kanner, B. I. (2005) Sulfhydryl modification of cysteine mutants of a neuronal glutamate transporter reveals an inverse relationship between sodium-dependent conformational changes and the glutamate-gated anion conductance. *Neuropharmacology* **49,** 862–871
45. Brocke, L., Bendahan, A., Grunewald, M., and Kanner, B. I. (2002) Proximity of two oppositely oriented reentrant loops in the glutamate transporter GLT-1 identified by paired cysteine mutagenesis. *J. Biol. Chem.* **277,** 3985–3992
46. Focke, P. J., Moenne-Loccoz, P., and Larsson, H. P. (2011) Opposite movement of the external gate of a glutamate transporter homolog upon binding cotransported sodium compared with substrate. *J. Neurosci.* **31,** 6255–6262
47. Grewer, C., Watzke, N., Wiessner, M., and Rauen, T. (2000) Glutamate translocation of the neuronal glutamate transporter EAAC1 occurs within milliseconds. *Proc. Natl. Acad. Sci. U.S.A.* **97,** 9706–9711
48. Otis, T. S., and Kavanaugh, M. P. (2000) Isolation of current components and partial reaction cycles in the glial glutamate transporter EAAT2. *J. Neurosci.* **20,** 2749–2757
49. Auger, C., and Attwell, D. (2000) Fast removal of synaptic glutamate by postsynaptic transporters. *Neuron* **28,** 547–558
50. Schicker, K., Uzelac, Z., Gesmonde, J., Bulling, S., Stockner, T., Freissmuth, M., Boehm, S., Rudnick, G., Sitte, H. H., and Sandtner, W. (2012) Unifying concept of serotonin transporter-associated currents. *J. Biol. Chem.* **287,** 438–445
51. Felts, B., Pramod, A. B., Sandtner, W., Burbach, N., Bulling, S., Sitte, H. H., and Henry, L. K. (2014) The two Na^+ sites in the human serotonin transporter play distinct roles in the ion coupling and electrogenicity of transport. *J. Biol. Chem.* **289,** 1825–1840
52. Li, J., Shaikh, S. A., Enkavi, G., Wen, P. C., Huang, Z., and Tajkhorshid, E. (2013) Transient formation of water-conducting states in membrane transporters. *Proc. Natl. Acad. Sci. U.S.A.* **110,** 7696–7701